Water Research 125 (2017) 23–31

Contents lists available at ScienceDirect

Water Research

journal homepage: www.elsevier.com/locate/watres

CO_2 saturated water as two-phase flow for fouling control in reverse electrodialysis

J. Moreno [a, b], N. de Hart [a], M. Saakes [a], K. Nijmeijer [b, *]

[a] Wetsus, European Centre of Excellence for Sustainable Water Technology, Oostergoweg 9, 8911MA, Leeuwarden, The Netherlands
[b] Membrane Science & Technology, University of Twente, P.O. Box 217, 7500AE, Enschede, The Netherlands

ARTICLE INFO

Article history:
Received 27 March 2017
Received in revised form
4 July 2017
Accepted 6 August 2017
Available online 9 August 2017

Keywords:
Salinity gradient energy
Reverse electrodialysis
Fouling
CO_2 nucleation
Two-phase flow

ABSTRACT

When natural feed waters are used in the operation of a reverse electrodialysis (RED) stack, severe fouling on the ion exchange membranes and spacers occurs. Fouling of the RED stack has a strong influence on the gross power density output; which can decrease up to 50%. Moreover, an increase in the pressure loss occurs between the feed water inlet and outlet, increasing the pumping energy and thus decreasing the net power density that can be obtained. In this work, we extensively investigated the use of CO_2 saturated water as two-phase flow cleaning for fouling mitigation in RED using natural feed waters. Experiments were performed in the REDstack research facility located at the Afsluitdijk (the Netherlands) using natural feed waters for a period of 60 days. Two different gas combinations were experimentally investigated, water/air sparging and water/CO_2 (saturated) injection. Air is an inert gas mixture and induces air sparging in the stack. In the case of CO_2, nucleation, i.e. the spontaneous formation of bubbles, occurs at the spacer filaments due to depressurization of CO_2 saturated water, inducing cleaning.

Results showed that stacks equipped with CO_2 saturated water can produce an average net power density of 0.18 W/m^2 under real fouling conditions with minimal pre-treatment and at a low outside temperature of only 8 °C, whereas the stacks equipped with air sparging could only produce an average net power density of 0.04 W/m^2. Electrochemical impedance spectroscopy measurements showed that the stacks equipped with air sparging increased in stack resistance due to the presence of stagnant bubbles remaining in the stack after every air injection. Furthermore, the introduction of CO_2 gas in the feed water introduces a pH decrease in the system (carbonated solution) adding an additional cleaning effect in the system, thus avoiding the use of environmentally unwanted cleaning chemicals.

1. Introduction

When seawater and river water are mixed, energy can be generated. The Gibb's Free Energy of Mixing calculated via the molar entropy change represents the amount of energy that can be harvested (Post et al., 2008; Weinstein and Leitz, 1976). Reversed electrodialysis (RED) is a technology to capture this energy, consisting of a system with cation exchange membranes (CEMs) and anion exchange membranes (AEMs) placed in alternating order. Between the membranes net-spacers are placed in order to create flow compartments. The flow compartments are alternately fed with waters of high and low salinity. This generates an electrical potential difference over the membranes as AEMs only allow the diffusion of anions and CEMs only allow the diffusion of cations. The RED stack is closed on both ends with an electrode system; a redox reaction converts the ionic transport into an electrical current that can be used to power an electrical device.

When natural feed waters are used, fouling on ion exchange membranes and spacers is a causes a major problem and decreases the performance of the RED stack. Different types of fouling can occur such as scaling, biofouling, adhesion of organic substances, and deposition of colloids (Vermaas et al., 2013). Both CEMs and AEMs are subject to different types of fouling, which is mainly related to the difference in charge of the membranes, AEMs are positive and CEMs are negative, and oppositely charged species are attracted to their surfaces. In general CEMs are mostly affected by scaling whereas AEMs are predominantly affected by organic

* Corresponding author. Current address: Membrane Materials and Processes, Eindhoven University of Technology, P.O. Box 513, 5600 MB, Eindhoven, The Netherlands.
E-mail address: D.C.Nijmeijer@tue.nl (K. Nijmeijer).

http://dx.doi.org/10.1016/j.watres.2017.08.015

fouling and colloidal fouling (Vermaas et al., 2014). Colloidal fouling and scaling clog the feed water channels and consequently increase the pressure drop along the feed compartments and deteriorate the flow distribution.

Fouling of the RED stack has a strong influence on the power density output, which can be decreased up to 60% (Vermaas et al., 2014). Moreover, an increase in pressure drop occurs between the feed water inlet and outlet, increasing the pumping energy and thus decreasing the net power density that can be obtained (Vermaas et al., 2013). The use of environmentally persistent chemical cleaning agents is not an option, as next to not being always effective, it also shortens membrane lifetime. In addition, RED uses natural water resources and environmentally persistent chemical agents should be avoided. As an alternative physical cleaning methods, such as two-phase flow cleaning, are often applied in membranes processes. Two-phase flow cleaning for fouling mitigation is widely used in e.g. microfiltration (MF), ultrafiltration (UF), nanofiltration (NF), reverse osmosis (RO) and electrodialysis (ED) (Cornelissen et al., 2007), and has also been investigated for application in RED (Vermaas et al., 2013). In membrane processes, gas/liquid two-phase flow is intentionally used to create hydrodynamic instabilities to disturb concentration polarization, to sweep away formed cake layers and to remove biofouling from membrane surfaces or net-spacers (Wibisono et al., 2014). Air is the most common gas mixture used in two-phase flow as it is omnipresent and easy to store and handle. In RED the use of water/air sparging has been studied by Vermaas et al. (2013) using profiled membranes that integrate the membrane and spacer functionality. During the experiment, the stack with air sparging as the antifouling strategy maintained a low pressure drop over the full duration of the experiment (67 days) in comparison to the stack without any antifouling strategy. Unfortunately, the authors only investigated the effect of two-phase flow using profiled membranes and did not consider the effectiveness of this approach in stacks with separate membranes and spacers. Profiled membranes are however not yet commercially available and the use of separate membranes and spacers in RED is initially foreseen for large-scale applications. Usually, woven net-spacers are used in RED to keep the membranes separated and create flow channels, since these are commercially produced and are in general thinner than extruded spacers. However, woven net-spacers are not desirable when using two-phase flow approaches as the gas introduction easily breaks the net-spacer structure, thus blocking the feed flow compartments.

Although the use of air bubbles in net-spacer filled channels with low liquid flow velocities is used in other membrane processes, such as NF and RO, one of the major drawbacks is that the introduction of air in the system results in the presence of undesired stagnant bubbles (Willems et al., 2009). These stagnant bubbles reduce the active membrane surface area available for water permeation (Willems et al., 2009) and ion diffusion in RED (Hatzell and Logan, 2013). Additionally, in RED the presence of stagnant bubbles in the stack induces an increase of the stack ohmic resistance, thus reducing the gross power density output of the system. In other words, the presence of stagnant bubbles reduces the amount of energy that potentially can be harvested (Hatzell and Logan, 2013). Although air is a very versatile choice for two-phase flow, it has a relatively low solubility in water (0.023 g/L at 1 atm at 25 °C, calculated using Henry's law) (Burton et al., 2013). This low solubility does not only limit the effectiveness of two-phase flow cleaning, it also increases the formation of stagnant bubbles. Carbon dioxide (CO_2), which has a solubility in water two orders of magnitude higher than that of air in water (1,27 g/L at 1 atm at 25 °C, calculated using Henry's law), is considered to be much more effective (Burton et al., 2013; Carroll et al., 1991). Ngene et al., 2010 investigated the use of CO_2 as antifouling strategy in reverse osmosis with spacer-filled channels. CO_2 was dissolved in water at a pressure higher than the working pressure used in the membrane process, meaning that upon entrance of the membrane module, the water was supersaturated in CO_2. This provokes CO_2 bubbles to nucleate due to depressurization. This CO_2 nucleation effect, i.e. the spontaneous formation of bubbles, happens at the spacer filaments due to local pressure differences, similar to the effervescence experienced upon opening carbonated drinks. Once the CO_2 saturated water leaves the spacer-filled channel the CO_2 gas is no longer dissolved in water and is released into the atmosphere, thus not inducing permanent changes in the natural system. In addition, the introduction of CO_2 in water (creating a carbonated solution) induces a pH decrease in the system and adds a beneficial cleaning effect i.e. a kind of chemical cleaning-in-place (CIP) (Partlan and Ladner, 2014).

In the present work, the effectiveness of CO_2 saturated water as a method for two-phase flow cleaning in RED is investigated and compared to a system with air sparging. For that we investigate the use of CO_2 saturated water as two-phase flow cleaning in a full scale REDstack system located at the Afsluitdijk (The Netherlands) using natural feed waters for a period of 60 days. Two different gas combinations are experimentally investigated: water/air sparging and water/CO_2 sparging. The results are compared to those of a stack without any cleaning strategy. The pressure drop over the inlet and outlet is measured using pressure meters and the gross power density is determined using chronopotentiometry. The net power density is subsequently calculated by subtracting the hydraulic resistance, expressed as the pressure drop over the inlet and the outlet of the feed water compartments multiplied by their respective flow rates, from the gross power density. In order to address the presence of stagnant and trapped CO_2 bubbles in the system, a separate experiment using the same conditions but artificial river and seawater is performed in the laboratory by measuring the ohmic resistance of the stack in time using electrochemical impedance spectroscopy (EIS). SEM analysis for fouling characterization is performed to visualize the deposited fouling.

2. Materials and methods

2.1. Stack configuration

A RED stack (Fig. 1) was built using housing supplied by REDstack BV (The Netherlands). The stack was composed of 5 cell pairs with CEM and AEM membranes (Neosepta CMX/AMX, Tokuyama Inc., Japan). Extruded polypropylene spacers with a thickness of 480 μm (Conwed, USA) were used to maintain the inter-membrane distance and to create the feedwater compartments (see Fig. 1). The spacers were coated with a dense silicon rubber layer as sealing at the sides (Deukum, Germany). An extra CEM was used to shield the electrolyte compartment. Titanium electrodes (mesh 1.7 m^2/m^2, area 96.04 cm^2) with a mixed ruthenium/iridium mixed oxide coating (Magneto Special Anodes BV, The Netherlands) were placed at both sides of the membrane pile.

A solution of 0.05 M $K_3Fe(CN)_6$, 0.05 M $K_4Fe(CN)_6$ and 0.25 M NaCl in demineralized water was circulated through the electrolyte compartments by an adjustable peristaltic pump (Cole-Parmer, Masterflex L/S Digital drive, USA) with a flow rate of 150 ml/min. The electrolyte was kept under a slight overpressure of 0.5 bar to avoid bulging of the feedwater compartments. For the fouling experiments with feed waters, five identical stacks were built. Pressure drop measurements were performed with a pressure difference transmitter (Endress + Hauser, type Deltabar S, Germany). The pressure drop values were recorded every 60 s using a data logger (Endress + Hauser, Ecograph T, Germany). The pH was

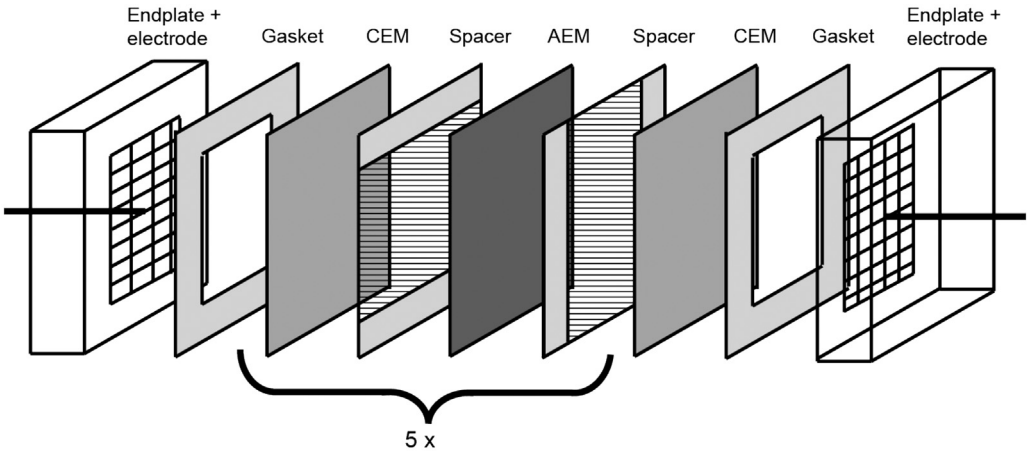

Fig. 1. Schematic illustration of the used cross-flow stack with spacers. For clarity, the figure contains only one representative CEM/AEM membrane pair but in the experiments, stacks with 5 cell pairs were used.

measured at the feed water outlets (river water and seawater) of the stacks using two pH sensors (Endress + Hauser, Memo Sens, Germany) and recorded every second using a data logger (Endress + Hauser, RSG 30, Germany).

2.2. Feed waters

To investigate the presence of stagnant and trapped air and CO_2 bubbles in the system, a separate experiment conducted under laboratory conditions using the same stack configuration was performed. For these experiments under laboratory conditions, artificial seawater and river water were used with a concentration of 0.507 M (30 g NaCl per kg water) and 0.017 M (1 g NaCl per kg water), respectively. These solutions were made with NaCl (technical grade, ESCO, The Netherlands) dissolved in demineralized water. During the experiments in the laboratory, the solutions were kept at 25 °C ± 0.5 °C with a heater (Tetratec HT300, Germany) and a pump. The artificial solutions were pumped through the stack by using two peristaltic pumps (Cole-Parmer, Masterflex L/S Digital drive, USA). Measurements were performed at 150 ml/min which equals a flow velocity of 1 cm/s.

Fouling experiments with real river and seawater were conducted at the REDstack Blue Energy research facility located at the Afsluitdijk, The Netherlands. Seawater intake is located at the Wadden Sea (Breezanddijk, The Netherlands) and the river water intake is located at the nearby lake (IJsselmeer, The Netherlands). In this paper, the mentioned sources are referred to as seawater and river water, respectively. Both feed waters were filtered through drum filters with a median diameter of 20 μm. Averaged water quality characteristics during the time of the experiment are shown in Table 1. The content of cation and anions was determined by ion chromatography (Metrohm Compact IC Flex 930, Schiedam, The Netherlands). The determination of total carbon and inorganic carbon was done using a Shimadzu TOC-L TOC analyser (Japan).

2.3. Injection of two-phase flow

Two different gases were used during the experiment, air and CO_2. Air was supplied from a compressor (Airpress, HLO 215,25, The Netherlands) and CO_2 was supplied from a pressurized gas cylinder (Premier CO_2, Air Products, The Netherlands). Air was introduced together (co-flow) with the feed water directly in the stack but the CO_2 gas was first dissolved in water in a separate vessel, until reaching saturation. To do so, CO_2 gas was bubbled for 10 min through a vessel filled with demineralized water to strip other dissolved gases from the water while also carbonating the demineralized water. Afterwards, the vessel was pressurized at 0.5 bar CO_2 overpressure to allow for saturation. The pH of the solution was measured using a pH sensor (Endress + Hauser, Memo Sens, Germany) to ensure CO_2 gas saturation. The CO_2 saturated water injection in the stack was done via a Y-joint just before the feed inlet (co-flow) and an electronic valve (Bürkert, 0124, Germany) controlled with a Raspberry Pi (Raspberry Pi Foundation, United Kingdom), using an open source python code.

The water/air sparging combination as well as the water/CO_2 (saturated) combination were introduced into the stack at a slight over pressure of 0.5 bar. All 5 stacks under investigation have the same stack configuration but the cleaning protocol is different; two stacks were injected with water/CO_2 and two stacks were injected with water/air sparging. For each injected gas type two injection protocols were investigated; 6 s gas injection every 30 min and 3 intervals of 2 s (totally 6 s) gas injection every 30 min. One stack was kept without any antifouling strategy and served as a reference stack (blank).

Table 1
Overview of average natural river and seawater composition (location: Afsluitdijk, The Netherlands).

	Cations (mg/L)	Anions (mg/L)	Temperature (°C)	Organic compounds[a] (mg/L)
River water	Na^+: 70 ± 3 Mg^{2+}: 13 ± 1 Ca^{2+}: 58 ± 2	Cl^-: 113 ± 9 SO_4^{2-}: 51 ± 12	8.1 ± 2.3	TC: 35 ± 2 IC: 29 ± 2
Seawater	Na^+: 6770 ± 1087 Mg^{2+}: 753 ± 115 Ca^{2+}: 626 ± 207	Cl^-: 11,518 ± 1839 SO_4^{2-}: 1620 ± 300	8.6 ± 2.4	TC: 44 ± 11 IC: 32 ± 2

[a] TC: Total Carbon, IC: Inorganic Carbon.

2.4. Electrochemical measurements

During laboratory experiments, electrochemical impedance spectroscopy (EIS) with an alternating sinusoidal signal of 5 kHz was applied to derive the stack ohmic resistance under open circuit voltage conditions (Moreno et al., 2016). About one hundred analyses per second were performed and the real component of the impedance was used to extract the ohmic resistance using a potentiostat (Ivium Technologies, The Netherlands).

During the fouling experiments, chronopotentiometry series were applied using the same potentiostat connected to a peripheral differential amplifier to measure the open circuit voltage, stack resistance and gross power density. The chronopotentiometry series was applied in cycles of 30 min (Fig. 2), however, most of the time a constant current of 2.5 A/m^2 was applied to simulate constant energy production. The constant current was interrupted during 200 s for the gas injection and after the gas injection the constant current was applied again.

The gross power density was derived from the potential at open circuit voltage (E_{OCV}), the stack area resistance and the total membrane area according to:

$$P_{gross} = \frac{{E_{OCV}}^2}{4 \cdot R_{stack} \cdot N_m} \quad (1)$$

in which P_{gross} is the power density (W/m^2), R_{stack} is the stack area resistance (Ω m^2) and N_m is the number of membranes in the stack (−). The stack area resistance was calculated from the steady state voltages during open circuit operation and during the stages with electrical current (2.5 A/m^2, 5.0 A/m^2 and 7.5 A/m^2), using Ohm's law (Vermaas et al., 2013).

The net power density was calculated by subtracting the energy consumed by pumping the feed waters from the gross power density:

$$P_{net} = \frac{{E_{OCV}}^2}{4 \cdot R_{stack} \cdot N_m} - \frac{\Delta p_{sea} \cdot \Phi_{sea} + \Delta p_{river} \cdot \Phi_{river}}{N_m \cdot A} \quad (2)$$

in which Δp is the pressure drop (Pa) over the inlet and outlet of the feedwater, Φ is the flow rate (m^3/s) of the feedwater and A is the area of one membrane (m^2).

2.5. Fouling experiments using real feed waters

The fouling experiments are divided in 3 periods. During period I (with a duration 30 days), the investigated antifouling strategies were applied to avoid the fouling accumulation into the stacks. After 30 days, the antifouling strategies were stopped for a period of 15 days, this is period II. The aim of disconnecting the antifouling strategies is twofold; to compare the results with period I and to investigate if the stacks could recover from a period without antifouling measures. During period III, the investigated antifouling strategies were re-started at day 45 and last until day 60 (15 days). During fouling experiments, an automatic backpressure valve was used to increase the pressure of the stacks subject to water/air sparging (see Supporting Information S1).

At the end of the fouling experiments, an autopsy of the stacks was performed. A visual and microscopic inspection of the fouled ion exchange membranes and spacer samples was performed using scanning electron microscopy (SEM; JEOL JSM-6480 LV, USA) and energy dispersive X-ray spectroscopy (EDX) (Oxford Instruments x-act SDD, UK).

3. Results and discussion

3.1. Two-phase flow injection under laboratory conditions

To investigate the possible presence of stagnant bubbles in the stacks, first laboratory experiments were performed using artificial river and seawater. The stack ohmic resistance was measured for the stacks with gas injection. The stack ohmic resistance includes the resistance of the feed water compartments, the membrane resistances and the spacer shadow effect of the spacers and the resistances of the electrode compartments. The ohmic resistance of the stack was measured before and after gas injection and the difference in ohmic resistance was attributed to the effect of gas bubbles inside the stack. In Fig. 3 the experimentally measured ohmic resistance at time intervals of 0.01 s for the different stack configurations is plotted against the time. As a reference starting point, first the stationary ohmic resistance is measured during 60 s. Gas injection is performed at time 60 s.

In Fig. 3a, corresponding with the stack with 3 × 2 s water/air sparging injection, a permanent increase in ohmic resistance after gas injection in the stack is visible. The same response is observed in Fig. 3b for the stack with 1 × 6 s water/air sparging. Even after a certain recovery time, the final stack ohmic resistances of these air-sparged stacks remain higher than the resistances measured at the start of the experiment. This increase in stack ohmic resistance is attributed to the presence of stagnant air bubbles remaining in the system, decreasing the conductivity of the feed water compartments, since air is less conductive than water. By increasing the stack backpressure up to 400 mbar during 2 s, air bubbles were observed to leave the stack at the exit of the feed water streams (see Supporting Information) resulting in a stack ohmic resistance decrease in again. This confirms that the increase in stack ohmic resistance is due the presence of stagnant air bubbles (Hatzell and Logan, 2013).

In Fig. 3c and d, corresponding with the injection of 3 × 2 s water/CO_2 (saturated) and 1 × 6 s water/CO_2 (saturated), respectively, a momentarily increase of the ohmic resistance to 10 Ω is

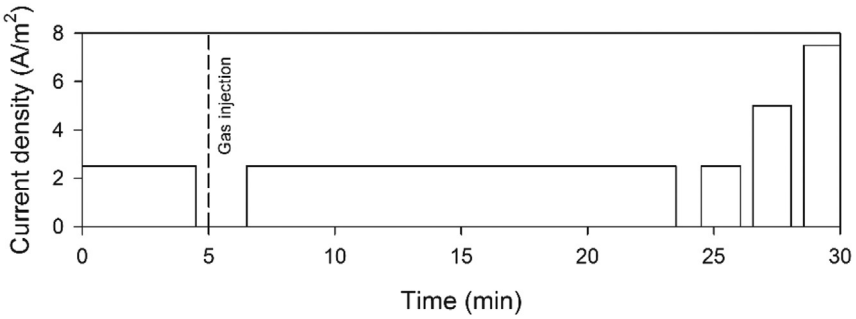

Fig. 2. Experimentally applied current density cycle over a repetitive period of 30 min.

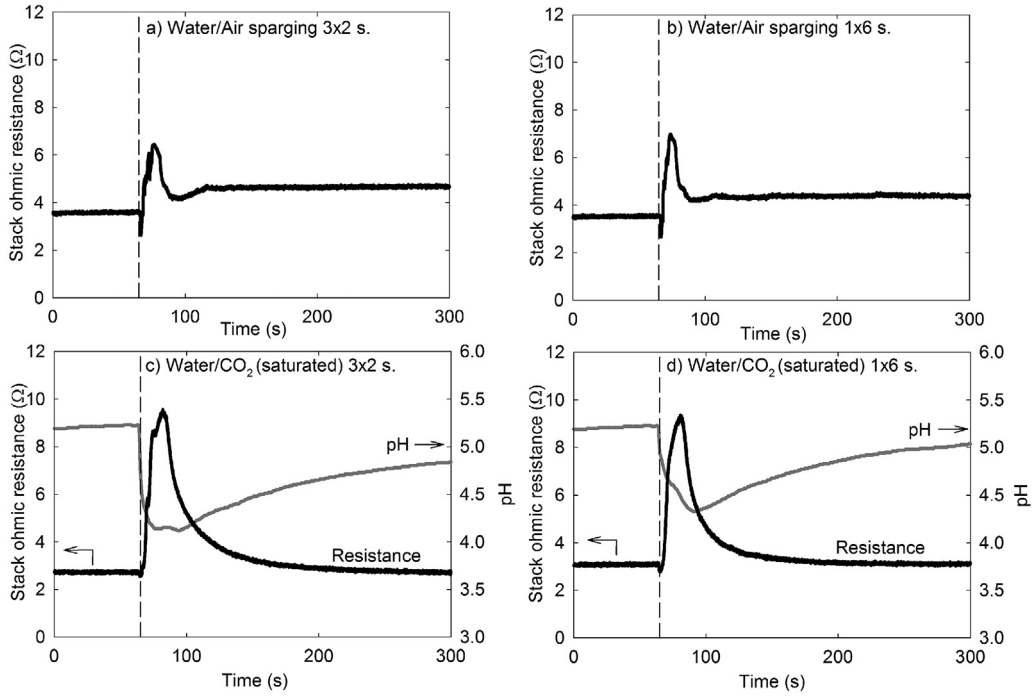

Fig. 3. Stack ohmic resistance as a function of time for a) water/air sparging injection 3 × 2 s, b) water/air sparging injection 1 × 6 s, c) water/CO_2 (saturated) injection 3 × 2 s, d) water/CO_2 (saturated) injection 1 × 6 s. Gas injection was performed at t = 60 s (vertical dashed line).

observed during 130 s after gas injection. After this increase in stack ohmic resistance, the values return to the initial stack ohmic resistance values before the gas injection. This behaviour is opposite to what is observed in stacks with air sparging, indicating that CO_2 bubbles do not remain trapped in the stack as compared to the stacks with air sparging injection. Consequently, the increase in stack ohmic resistance after CO_2 injection is not permanent. However, the initial stack ohmic resistance increase after water/CO_2 (saturated) injection is higher than the one observed for water/air sparging injection. The reason is that demineralized water (which has a lower conductivity) was used to prepare the water/CO_2 solution used for injection. Once the feed compartments are refreshed with river and seawater (residence time is 10 s), the stack ohmic resistance values is recovered towards the original value before the gas injection.

Furthermore, after the injection of water/CO_2 (saturated), an additional effect is observed: i.e. a pH decrease. This is due the dissolution of CO_2 gas. In Fig. 3c, corresponding to 3 × 2 s water/CO_2 (saturated) injection, the pH drop lasts longer than for the stack with 1 × 6 s water/CO_2 (saturated) injection. This is particularly interesting since the chemical cleaning effect can be more effective due to the change in pH and at higher residence times of the water/CO_2 (saturated) inside the stack. The stacks with water/air sparging injection did not experience a decrease in pH during the gas injection and the pH kept a constant value of 5.2 ± 0.4.

3.2. Fouling experiments using real feed water

3.2.1. Pressure drop

Experiments with real river and seawater at the Afsluitdijk were performed using four stacks with gas sparging (two with air, two with CO_2) and one reference stack without any cleaning measures. The feed spacer channel pressure drop, i.e. the pressure drop between the inlet and the outlet of the feed water compartments, gives information about the accumulated fouling in the feed compartment. An increase in pressure drop means increased hydraulic losses, therefore increasing the pumping energy needed to pump the feed waters. The occurrence of fouling induces an increase in pressure drop and is an undesired effect as it is a prerequisite to keep the pumping energy as low as possible. Time series for the average pressure drop over the feed water compartments for all stack configurations are presented in Fig. 4.

During period I (30 days with water/air or water/CO_2 (saturated) injection), the stacks with water/CO_2 (saturated) injection showed a slightly lower average pressure drop than the stacks with air injection. For both stacks with water/CO_2 (saturated) injection, the values are below 20 mbar. The stack with 1 × 6 s water/air sparging always shows a higher average pressure drop than the stack with 3 × 2 s water/air sparging. The blank stack (reference stack without

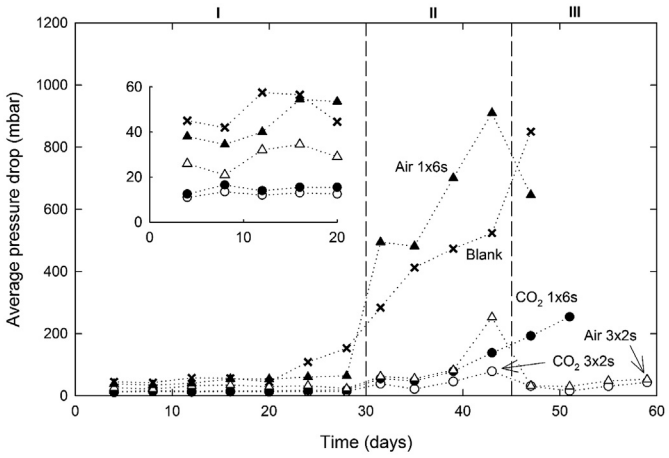

Fig. 4. Average pressure drop over the feed water compartments plotted against the time after the start of the experiment for all stacks. The symbols indicate (●): CO_2 1 × 6 s; (○): CO_2 3 × 2 s; (▲): Air 1 × 6 s; (Δ): Air 3 × 2 s and (x): Blank.

antifouling strategy) gives the highest pressure drop during this period. Especially during the first 20 days, differences are small as fouling needs a certain induction time. However, after that, the stack without gas sparging clearly shows a strong increase in pressure drop and consequently fouling.

In the second period (II), all antifouling strategies were terminated for a period of 15 days. During this period the effect of fouling is clearly visible in all stacks; however, the stacks with water/CO_2 (saturated) injection during the first stage, maintain low average pressure drop values. On the other hand, both the stack with water/air sparging injection of 1 × 6 s and the blank stack clearly show a strong increase in pressure drop from 100 mbar to 1000 mbar in only 15 days. This results in pressure drops (and thus pumping power losses) that are an order of magnitude higher for the blank and for the water/air sparging of 1 × 6 s than those of the stacks with the other antifouling strategies. Due to the introduction of air in the stack, stagnant air bubbles remain in the stack as was proven with the laboratory experiments. Membrane autopsy using SEM revealed a dry fouling layer in the corners of these stacks (see Supporting Information). The stack with 3 × 2 s of water/air sparging also showed some of these dried residues in the corners, but these were not as severe as the ones in the stack with 1 × 6 s of water/air sparging. These dry residues result in the formation of a dry cake layer on top of the membrane, thus reducing the compartment volume and severely increasing the pressure drop over the inlet and the outlet of the stack. The stacks injected with CO_2 saturated water did not show dried deposits, most likely because the gas is first dissolved in water and subsequently injected, preventing the formation of stagnant air bubbles. The pressure drop in the blank stack continued to increase, as expected, since no antifouling strategy was implemented. The pressure drop of all stacks immediately started to increase as soon as the antifouling strategies were stopped, implying that during stack operation antifouling strategies need to be continuous and permanent.

During the last period (III), the different antifouling strategies were started again. Only the stacks with a pulsed injection of 3 × 2 s (for both air and CO_2), recovered to the initial performance values in terms of pressure drop. Most probably, the pulsation adds an extra shear force and pushes out the deposited fouling. The stack with air sparging at a frequency of 1 × 6 s was stopped as the high pressure drop in the flow water compartments resulted in heavy leakage of electrolyte solution. Also, the stack without any sparging was stopped due to the high and continuously increasing pressure drop.

3.2.2. Gross power density

In Fig. 5 the gross power density as a function of time for all stack configurations is presented.

During the first period (I), the blank stack shows the lowest gross power density values, since no antifouling strategies are applied. These low gross power densities are the consequence of fouling inside the flow compartments. The stacks with the water/CO_2 (saturated) antifouling strategy show higher gross power density values than the stacks with water/air sparging. An increase in stack resistance decreases the gross power density output, as resistance represents loss. This increase in resistance can have two causes; the deposition of fouling and the presence of stagnant bubbles. The four stacks with antifouling strategies all show a different gross power density, whereas the pressure drop is almost equal in all cases (Fig. 4). This indicates that lower gross power densities for the stacks with air sparging are mostly the consequence of stagnant bubbles in the stack, as confirmed by the laboratory experiments and in the Supporting Information. The slightly lower pressure drop values of the water/CO_2 (saturated) stacks and the absence of bubbles and dried fouling residues combined with CO_2 nucleation and the effect of pH decrease make

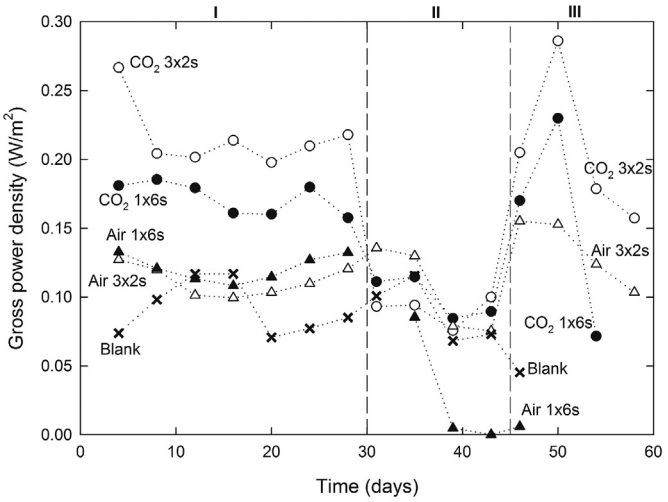

Fig. 5. Gross power density plotted against the time after the start of the experiment for all stacks. The symbols indicate (●): CO_2 1 × 6 s; (○): CO_2 3 × 2 s; (▲): Air 1 × 6 s; (Δ): Air 3 × 2 s and (x): Blank.

this cleaning strategy more effective compared with water/air sparging. This is in agreement of other authors (Partlan and Ladner, 2014).

During the second period (II) all stacks give lower gross power density values than during the first period (I), except for the blank stack. Especially the stack with water/air sparging with an injection protocol of 1 × 6 s has a low performance, as expected, because of the aforementioned presence of dry residues in the feed compartments and stagnant bubbles. The rest of the stacks showed a gradual decrease in gross power output due to increasing pressure drops with time, indicating the need of antifouling strategies in order to harvest energy form the salinity gradient.

During the last period (III), initially during the first 5 days (day 45 to day 50) a slight increase in power outputs was observed for all stacks, but after those days the values drop again. This general increase in power density during the first five days is not related to the anti-fouling strategies applied, but the consequence of a temporary episode of strong winds at the research facility location. These strong North-Western winds bring highly saline waters from the North Sea to the Wadden Sea, and thus temporarily increase the salinity gradient. After that, the stack with 1 × 6 s air sparging and the stack without any sparging show a strong decrease in power output with time, while all other stacks show a slight decrease in power density with time. CO_2 sparging thus shows to be effective in reducing fouling, although it cannot be avoided completely. Also, 3 × 2 s is more effective than 1 × 6 s.

3.2.3. Net power density

In Fig. 6 the net power density as function of time is presented for all stack configurations. The net power density is the resulting energy from subtracting the pumping energy from the obtained gross power density. The measured net power output values are low in comparison to earlier work. However, this is the consequence of the low temperatures of the waters (~8–8.5 °C) at this time of the year and the thick feed water compartments resulting in higher ohmic resistances when compared to previous work.

During the first period (I), the stacks equipped with water/CO_2 (saturated) as antifouling strategy give higher net power density values than the other stacks. The combination of a bubble-free stack, the additional effect of the CO_2 nucleation and pH drop and the low pumping energy consumed yields a reasonable net power

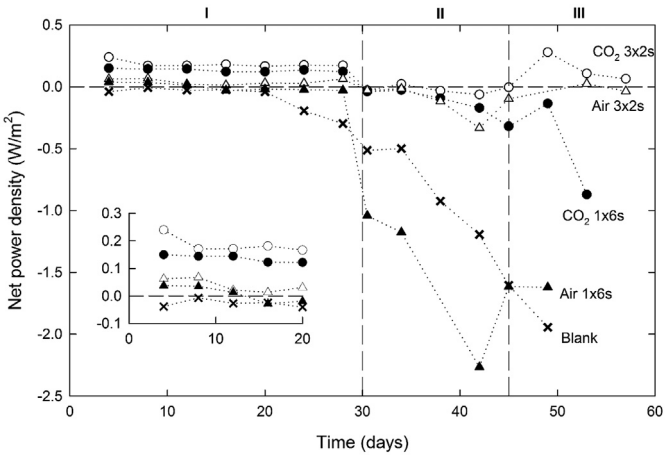

Fig. 6. Net power density plotted against time after the start of the experiment for all stacks. The symbols indicate (●): CO_2 1 × 6 s; (○): CO_2 3 × 2 s; (▲): Air 1 × 6 s; (Δ): Air 3 × 2 s and (x): Blank.

density value. In contrast, the stacks equipped with water/air sparging as antifouling strategy, perform worse. The effect of air bubbles remaining in the stacks and the low efficiency of the antifouling strategy contribute to this low net power density. The blank stack always consumes more pumping energy than it produces by salinity gradient energy, thus already in the first period resulting in a negative net power density.

During the second period (II), when no cleaning measures are applied, none of the stacks produces power, indicating the necessity of antifouling strategies at these feed water conditions (low temperatures and presence of divalent ions) and stack configurations (ca. 500 μm thick feed water compartments resulting in high ohmic stack resistances).

During the last period (III), only the stacks with pulsed injection (3 × 2 s) could recover and produce positive values for the net power density. The use of a pulsed injection turns out to be a more efficient way of removing fouling, due to the pulsating forces imposed on possible fouling deposits. The stack with 3 × 2 s of water/CO_2 (saturated) injection gives the highest net power density, followed by the stack with 3 × 2 s of water/air sparging. Opposite to this, the stack with 1 × 6 s of water/CO_2 (saturated) injection cannot recover from the period without cleaning measures. Even though the gross power density is slightly positive, the high pressure drop values counteract this, resulting in a negative net power production. The stack with 1 × 6 s of water/air sparging recovers to a certain extent when the antifouling strategy is restarted, mainly due to the decrease in pressure drop. The blank stack shows the lowest net power density values as fouling deposition continues.

After the fouling experiment (60 days) stacks were opened and examined visually and investigated by SEM and energy dispersive x-ray spectroscopy (EDX) to identify the chemical composition of the foulants. Fig. 8 shows photographic images of a representative spacer, an anion and a cation exchange membrane.

All stacks were fouled in a comparable way. Fouling was observed mostly in the seawater compartments and less in the river water compartments. Also, most of the foulants were observed on the AEMs while the CEMs were less fouled. Similar observations were made by previous authors (Vermaas et al., 2013) The seawater compartment net-spacers were fouled in an uneven form; the first part (0–2 cm out of 10 cm) of the net-spacers, corresponding to the entrance/inlet of the flow compartments, retained most of the deposited foulants (Fig. 8a). EDX measurements show that the deposited material is a mixture of clay (alumina silicates) and sand (silica oxides), which was not retained by the pre-treatment (i.e. 20 μm filter). The deposition of this material, just at the entrance, affects the stacks in two ways; firstly, the flow distribution of the water through the compartments is disturbed (not-uniform flow velocity), thus decreasing the obtainable gross power density. Secondly, blocking of the entrance contributes to an increase in pressure drop and thus pumping energy needed to flow the feed waters. This results in a lower net power density. The river compartment net-spacers were less fouled and fouling was hardly visible by the naked eye. The order of fouling of the different stacks matches very well with the order of the average pressure drop increase during the third operational period (III) (shown in the Supporting Information). The blank stack shows the strongest fouling, followed by the stack with 1 × 6 s water/air sparging with dried residues in the corners (Fig. 8c), the 1 × 6 s water/CO_2 (saturated) stack, then the 3 × 2 s water/air sparging stack and finally the 3 × 2 s water/CO_2 (saturated) stack, which shows the least amount of fouling. This order is in agreement with the order found for the increase in pressure drop and consequently, the change in pressure drop is a clear measure for the amount of fouling (Vermaas et al., 2014).

SEM images of ion exchange membranes a clearly shows the place where the spacers were positioned (Fig. 8a). Furthermore, in Fig. 8b is also clearly visible that fouling predominantly accumulates around the spacer filaments. SEM images confirm that AEMs are indeed more fouling sensitive than CEMs. The brownish colour observed in Fig. 7b suggests that foulants like humic acids are

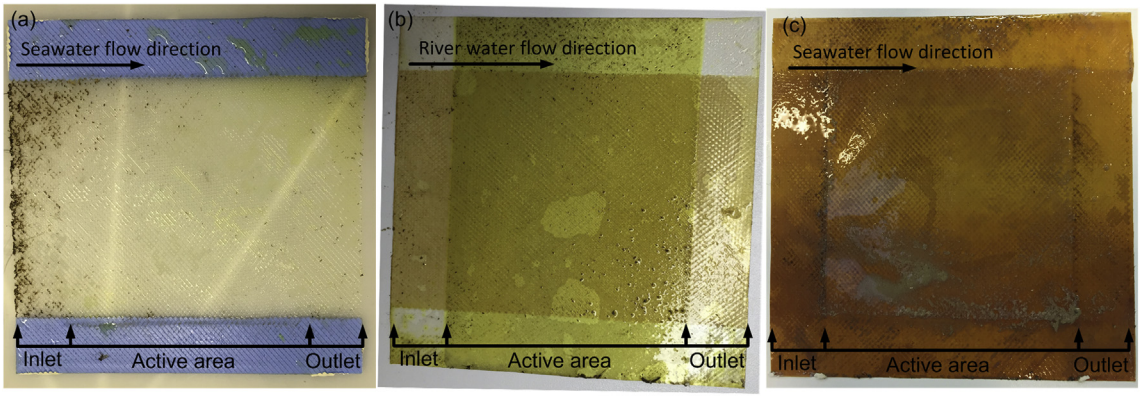

Fig. 7. Representative images from a) the seawater compartment net-spacer, b) the anion exchange membrane in contact with river water and c) the cation exchange membrane that was in contact with seawater with dry fouling residues in the corner.

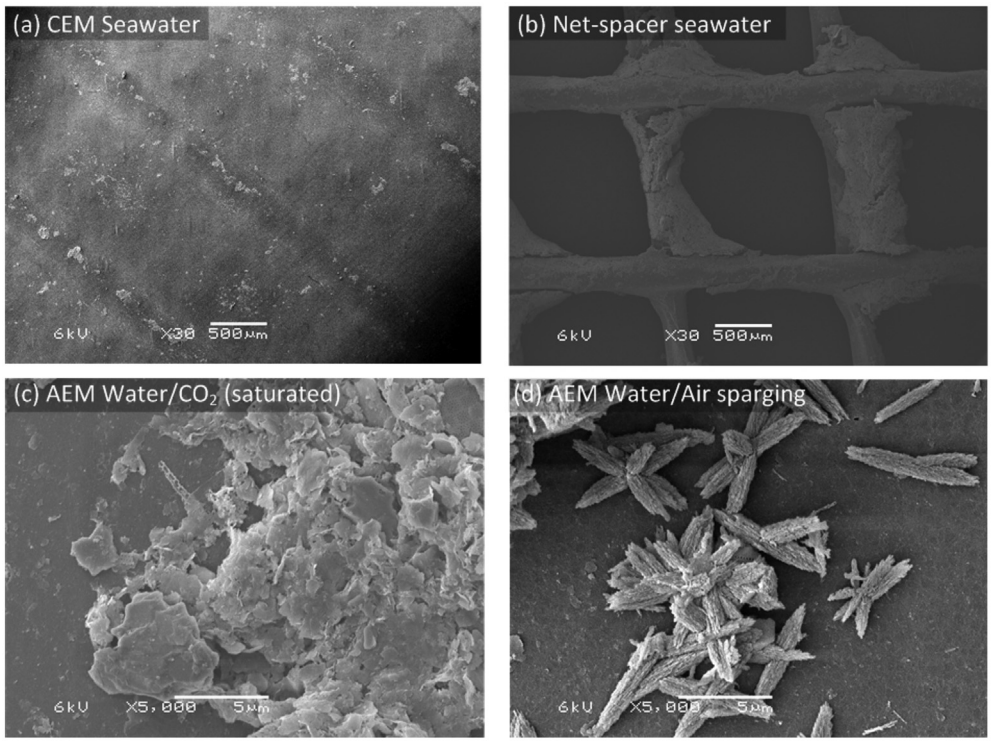

Fig. 8. SEM images of cation and anion exchange membranes (CEMs and AEMs) and net spacers in contact with seawater. a) and c) images are obtained from stack with 3 × 2 s water/CO_2 (saturated) strategy; b) and d) are obtained from the stack with 3 × 2 s water/air sparging strategy.

adsorbed on and absorbed in the membrane material (Vermaas et al., 2013). The EDX analysis of the ion exchange membranes showed a mixture of foulants on the membrane surfaces, like clay, sand, diatoms remnants (silica-based skeletons), precipitated calcium carbonates ($CaCO_3$) and magnesium carbonates ($MgCO_3$). Calcium carbonates and magnesium carbonates were only observed inside stacks equipped with water/air sparging and the blank (Fig. 8d). The stacks with water/CO_2 (saturated) did not have any calcium carbonate nor magnesium carbonate crystals precipitates (Fig. 8c). This is a consequence of the pH drop of the feed due to the injection of CO_2 saturated water injection. The low pH value (ca. ~4.5) achieved every 30 min upon CO_2 injection is apparently sufficient to dissolve these carbonated residues, resulting in a more effective cleaning of the membranes (Partlan and Ladner, 2014).

4. Conclusions

CO_2 saturated water has been used successfully as two-phase flow cleaning and fouling control in reverse electrodialysis. The results show that the stacks equipped with CO_2 saturated water can produce an average net power density of 0.18 W/m^2 under real fouling conditions at a low feed water temperature of only ~8–8.5 °C and with very thick feed water compartments and thus high resistances, whereas the stacks equipped with air sparging could only produce an average net power density of 0.04 W/m^2 under the same conditions. There are two main reasons for the more effective fouling control of the stack with water/CO_2 (saturated) injection; EIS measurements show that the stacks equipped with air sparging increase in stack resistance due to the presence of stagnant bubbles remaining in the stack after every air sparging injection. This does not occur in the case were water/CO_2 (saturated) is injected. In addition, the introduction of saturated water/CO_2 in the stack causes a nucleation effect and a significant decrease in feed water pH. Consequently, periodic pulsating injection of CO_2 is an effective method to decrease the effect of fouling, resulting in higher power densities compared to stacks without any anti-fouling measures or with air sparging as cleaning strategy.

Acknowledgements

This work was performed in the cooperation framework of Wetsus, European Centre of Excellence for Sustainable Water Technology (www.wetsus.eu). Wetsus is co-funded by the Dutch Ministry of Economic Affairs and Ministry of Infrastructure and the Environment, the Province of Fryslân, and the Northern Netherlands Provinces. The authors like to thank Dr. Olivier Schaetzle and Dr. Antoine Kemperman for the discussions and the participants of the research theme “Blue Energy” for the fruitful collaboration and their financial support.

Appendix A. Supplementary data

Supplementary data related to this article can be found at http://dx.doi.org/10.1016/j.watres.2017.08.015.

References

Burton, F., Tchobanoglous, G., Tsuchihashi, R., Stensel, H.D., Metcalf, Eddy, I., 2013. Wastewater Engineering: Treatment and Resource Recovery. McGraw-Hill Education.

Carroll, J.J., Slupsky, J.D., Mather, A.E., 1991. The solubility of carbon dioxide in water at low pressure. J. Phys. Chem. Ref. Data 20, 1201. http://dx.doi.org/10.1063/1.555900.

Cornelissen, E., Vrouwenvelder, J., Heijman, S., Viallefont, X., Vanderkooij, D., Wessels, L., 2007. Periodic air/water cleaning for control of biofouling in spiral wound membrane elements. J. Memb. Sci. 287, 94–101. http://dx.doi.org/10.1016/j.memsci.2006.10.023.

Hatzell, M.C., Logan, B.E., 2013. Evaluation of flow fields on bubble removal and system performance in an ammonium bicarbonate reverse electrodialysis stack.

J. Memb. Sci. 446, 449–455.
Moreno, J., Slouwerhof, E., Vermaas, D.A., Saakes, M., Nijmeijer, K., 2016. The breathing cell: cyclic intermembrane distance variation in reverse electrodialysis. Environ. Sci. Technol. 50, 11386–11393. http://dx.doi.org/10.1021/acs.est.6b02668.
Ngene, I.S., Lammertink, R.G.H., Kemperman, A.J.B., van de Ven, W.J.C., Wessels, L.P., Wessling, M., Van der Meer, W.G.J., 2010. CO_2 nucleation in membrane spacer channels remove biofilms and fouling deposits. Ind. Eng. Chem. Res. 49, 10034–10039. http://dx.doi.org/10.1021/ie1011245.
Partlan, E.T., Ladner, D.A., 2014. Removal of inorganic scale from RO membranes using dissolved CO_2. In: AWWA/AMTA 2014 Membrane Technology Conference and Exposition.
Post, J.W., Hamelers, H.V.M., Buisman, C.J.N., 2008. Energy recovery from controlled mixing salt and fresh water with a reverse electrodialysis system. Environ. Sci. Technol. 42, 5785–5790.
Vermaas, D.A., Kunteng, D., Saakes, M., Nijmeijer, K., 2013. Fouling in reverse electrodialysis under natural conditions. Water Res. 47, 1289–1298.
Vermaas, D.A., Kunteng, D., Veerman, J., Saakes, M., Nijmeijer, K., 2014. Periodic feedwater reversal and air sparging as antifouling strategies in reverse electrodialysis. Environ. Sci. Technol. 48, 3065–3073. http://dx.doi.org/10.1021/es4045456.
Weinstein, J.N., Leitz, F.B., 1976. Electric power from differences in salinity: the dialytic battery. Science 191 (80), 557–559.
Wibisono, Y., Cornelissen, E.R., Kemperman, A.J.B., van der Meer, W.G.J., Nijmeijer, K., 2014. Two-phase flow in membrane processes: a technology with a future. J. Memb. Sci. 453, 566–602. http://dx.doi.org/10.1016/j.memsci.2013.10.072.
Willems, P., Kemperman, A.J.B., Lammertink, R.G.H., Wessling, M., Annaland, M. van S., Kuipers, J.A.M., Deen, N.G., van der Meer, W.G.J., 2009. Bubbles in spacers: direct observation of bubble behavior in spacer filled membrane channels. J. Memb. Sci. 333, 38–44.